HUMAN GENE THERAPY 23:859–870 (August 2012)

DOI: 10.1089/hum.2011.123

Tissue Kallikrein Promotes Cardiac Neovascularization by Enhancing Endothelial Progenitor Cell Functional Capacity

Yuyu Yao,[1] Zulong Sheng,[1] Yefei Li,[1] Fengdi Yan,[1] Cong Fu,[1] Yongjun Li,[1] Genshan Ma,[1] Naifeng Liu,[1] Julie Chao,[2] and Lee Chao[2]

Abstract

Tissue kallikrein (TK) has been demonstrated to improve neovasculogenesis after myocardial infarction (MI). In the present study, we examined the role and underlying mechanisms of TK in peripheral endothelial progenitor cell (EPC) function. Peripheral blood-derived mononuclear cells containing EPCs were isolated from rat. The *in vitro* effects of TK on EPC differentiation, apoptosis, migration, and vascular tube formation capacity were studied in the presence or absence of TK, kinin B_2 receptor antagonist (icatibant), and phosphatidylinositol-3 kinase inhibitor (LY294002). Apoptosis was evaluated by flow-cytometry analysis using Annexin V-FITC/PI staining, as well as western-blot analysis of Akt phosphorylation and cleaved caspase-3. Using an MI mouse model, we then examined the *in vivo* effects of human TK gene adenoviral vector (Ad.hTK) administration on the number of $CD34^+Flk\text{-}1^+$ progenitors in the peripheral circulation, heart tissue, extent of vasculogenesis, and heart function. Administration of TK significantly increased the number of Dil-LDL/UEA-lectin double-positive early EPCs, as well as their migration and tube formation properties *in vitro*. Transduction of TK in cultured EPCs attenuated apoptosis induced by hypoxia and led to an increase in Akt phosphorylation and a decrease in cleaved caspase-3 levels. The beneficial effects of TK were blocked by pretreatment with icatibant and LY294002. The expression of recombinant human TK in the ischemic mouse heart significantly improved cardiac contractility and reduced infarct size 7 days after gene delivery. Compared with the Ad.Null group, Ad.hTK reduced mortality and preserved left ventricular function by increasing the number of $CD34^+Flk\text{-}1^+$ EPCs and promoting the growth of capillaries and arterioles in the peri-infarct myocardium. These data provide direct evidence that TK promotes vessel growth by increasing the number of EPCs and enhancing their functional properties through the kinin B_2 receptor-Akt signaling pathway.

Introduction

Recent studies have shown that improvement of neovascularization is a therapeutic option to rescue tissue from critical ischemia (Isner *et al*., 1999). Transplantation of *ex vivo* expanded endothelial progenitor cells (EPCs) or mobilization of $CD34^+$ cells by drugs was shown to improve cardiac function after myocardial ischemia (Kocher *et al*., 2001; Loomans *et al*., 2004). However, patients with diabetes, hypercholesterolemia, hypertension, and smoking have impaired EPC function, including decreased mobilization from the bone marrow and reduced incorporation into neovascular foci (Loomans *et al*., 2004). Additionally, EPC number is associated with endothelial function and the Framingham risk score (Hill *et al*., 2003). EPC number and function were shown to be improved by various cytokines and growth factors, such as vascular endothelial growth factor, stromal cell–derived factor-1, certain drugs, and physical exercise (Chavakis *et al*., 2008). Thus, EPC levels and functional capacity are important factors in cardiovascular and ischemic conditions.

The serine protease tissue kallikrein (TK) specifically processes low-molecular-weight kininogen to produce the potent vasoactive peptides bradykinin (BK) and Lys-bradykinin (kallidin) (Silva *et al*., 2000). The tissue kallikrein-kinin system (KKS) contributes to the revascularization of ischemic tissues (Madeddu *et al*., 2007). The effects of kallikrein and kinin on cardiac angiogenesis are mediated via kinin B_2 receptor (B_2R) activation, leading to the recruitment of circulating angiogenic progenitor cells to sites of ischemia and stimulating their proangiogenic action (Kränkel *et al*., 2008).

[1]Department of Cardiology, Zhongda Hospital, Medical School of Southeast University, Nanjing, Jiangsu 210009, China.
[2]Department of Biochemistry and Molecular Biology, Medical University of South Carolina, Charleston, SC 29425.

We have previously shown that local delivery of adenovirus carrying the human TK (hTK) gene (Ad.hTK) accelerates spontaneous angiogenesis and blood-flow perfusion in a rat model of myocardial infarction (MI) and induces arteriogenesis through the Akt-glycogen synthase kinase (GSK)-3β pathway (Yao *et al*., 2008). Thus, the KKS might play a role in multiple steps of postnatal vasculogenesis, as TK modulates EPC function and blood-vessel repair in response to injury.

In this study, we evaluated the effects of TK on EPC differentiation, apoptosis, migration, and vascular tube formation, as well as the possible molecular mechanisms involved. We also demonstrated the influence of TK on EPC numbers and on collateral vessel formation *in vivo* using a mouse MI model.

Materials and Methods

Preparation of replication-deficient adenoviral vectors

Adenovirus harboring the hTK cDNA (Ad.hTK) under the control of the cytomegalovirus enhancer/promoter and adenoviral vector alone (Ad.Null) were constructed and prepared as described previously (Yoshida *et al*., 2000).

EPC culture and differentiation

All procedures using rats and mice were performed in conformity with standards for the care and use of laboratory animals (Laboratory Animal Center of Southeast University). Peripheral blood-derived mononuclear cells (PBMCs) were isolated from healthy donor Sprague-Dawley rats (Shanghai Laboratory Animal Center of the Chinese Academy of Science) weighing 200 g. Ten milliliters of blood were collected from the left ventricle of anesthetized rats and diluted with an equal volume of PBS. PBMCs were then separated by density-gradient centrifugation using 1.077 g/ml Histopaque solution (Sigma, St. Louis, MO). Cells were seeded on fibronectin-coated tissue culture plates and maintained with endothelial growth media supplemented with EGM-2 Single Quots (Lonza, Walkersville, MD), as described previously (Yao *et al*., 2011).

Rat TK and BK were added to culture for a final concentration of 0.01 μM. At day 3 of culture, nonadherent cells were removed by thorough washing with PBS. Medium was changed after 3 additional days. After 7 days of culture, cells were incubated with 2.4 μg/ml 1,1-dioctadecyl-3,3,3′,3′-tetramethylindocarbocyanine–labeled acetylated low-density lipoprotein (Dil-Ac-LDL) (Invitrogen, Carlsbad, CA) for 1 hr and counterstained with fluorescein isothiocyanate (FITC)–labeled lectin from *Ulex europaeus* (UEA-1-lectin; Sigma). Cells were then examined under a fluorescence microscope. Cells presenting double-positive fluorescence were considered to be EPCs. After staining, the total number of double-positive Dil-Ac-LDL/UEA-1-lectin cells was calculated by counting cells in each field and was expressed as the percentage of EPCs positive for merged Dil-Ac-LDL/UEA-1-lectin dual staining, as described previously (Ebrahimian *et al*., 2006). Dil-Ac-LDL uptake and UEA-1-lectin binding staining of isolated EPCs from PBMCs untreated and treated with BK or TK for 7 days were determined by FACS-computed counting. Cells were incubated with Dil-Ac-LDL and trypsinized. Cells were fixed in 4% paraformaldehyde and counterstained with UEA-1-lectin. Quantitative fluorescence analysis was performed with a FACSCanto instrument (BD Biosciences, Rockville, MD).

Only third- or fourth-passage cells were used for further experiments. Immunocytofluorescence was used to analyze the expression of various progenitor (CD34, CD45) and endothelial lineage markers (KDR/Flk-1, CD31); antibodies against rat CD34 and CD45 (BD Biosciences) and KDR and CD31 (Santa Cruz Biotechnology, Santa Cruz, CA) were used as primary antibodies.

EPC migration assay

The migratory function of EPCs was evaluated by a modified Boyden chamber (Costar, Cambridge, MA) assay. In brief, after incubation with 1% serum medium for 24 hr, EPCs (passage 3) were seeded into six-well plates. Cells were transduced with Ad.hTK or Ad.Null at multiplicity of infection (MOI) 50 for 12 hr. EPCs were detached and then placed in the upper chamber of 24-well transwell plates (1×10^4 cells/well) with polycarbonate membrane (8-μm pores) with serum-free EGM-2 medium. In some experiments, cells were incubated with kinin B_2R antagonist icatibant (1 μM; Sigma) or phosphatidylinositol 3-kinase (PI3K) inhibitor LY294002 (10 μM ; Sigma). After incubation for 12 hr, the membrane was washed briefly with PBS. The upper side of the membrane was wiped gently with a cotton ball and then stained with 1% crystal violet in 2% ethanol. Results are presented as the percentage of seeded EPCs. All groups were studied in triplicate.

Matrigel tube formation assay

To analyze the capillary-like tube formation of EPCs, growth factor-reduced Matrigel (BD Biosciences, San Jose, CA) at 50 μl/well was laid into 96-well plates to solidify. EPCs (passage 3) were seeded into six-well plates. Cells were transduced with Ad.hTK or Ad.Null at MOI 50 for 12 hr. EPCs (1×10^4) were resuspended in 200 μl of EGM-2 without EGM-2 Single Quots supplements and plated on Matrigel. In some experiments, cells were incubated with icatibant or LY294002. After 18 hr, the mean tube length was calculated in three randomly chosen fields from each well ($\times$40) by Image-Pro Plus and was calculated against control groups.

EPC apoptosis assay

EPCs (passages 3 to 4) were seeded into six-well plates. After 48 hr, cells were transduced with Ad.hTK or Ad.Null at MOI 50 for 12 hr followed by 12-hr hypoxia (95% N_2 and 5% CO_2). In some experiments, EPCs were treated with icatibant or LY294002 for 30 min prior to hypoxia. Expression and localization of hTK in EPCs after Ad.hTK transduction were identified immunocytochemically using a rabbit anti-kallikrein antibody.

EPC apoptosis was evaluated with Annexin V-FITC/PI Apoptosis Detection Kit (BioVision Inc., Mountain View, CA). After treatment, the adherent and nonadherent cells were harvested with trypsin. The cells were then stained with Annexin-V-FITC and propidium iodide in 1 $\times$ binding buffer for 15 min at room temperature. Flow-cytometric analyses were performed on a FACS flow cytometer (Becton Dickinson, Heidelberg, Germany), and the data were analyzed by the Cell Quest analysis program.

Western-blot analysis

After treatment, the adherent and nonadherent cells were washed twice with PBS, lysed in lysis buffer [10 mmol/L Tris-HCl, pH 7.4, containing 1% Triton X-100, 100 mmol/L sodium chloride, 20 mmol/L sodium pyrophosphate, 2 mmol/L sodium orthovanadate, 2 mmol/L EDTA, and 1% protease inhibitor cocktail (Sigma)], and centrifuged at 12,000 *g* for 30 min at 4°C. The supernatant (the cytosolic fraction) was removed, and protein concentrations were measured by BCA assay (Pierce, Rockford, IL). Western-blot analysis was performed using the cytosolic fraction to detect cleaved caspase-3 and the total and phosphorylated forms of Akt (Cell Signaling, Danvers, MA). Western-blot analysis of GAPDH was used as a loading control (Advanced Immunochemical, Long Beach, CA). After incubation with primary antibody diluted in blocking buffer for 1 hr and washing, the blot was incubated for 30 min with appropriate secondary anti-IgG horseradish peroxidase conjugate. The membrane was washed three times for 5 min each and developed with SuperSignal chemiluminescent substrate (Pierce).

MI model and in vivo gene transfer

Male C57BL/6J mice (23 ± 0.1 g) were anesthetized with sodium pentobarbital (50 mg/kg, i.p.) and intubated before being subjected to ligation of the left coronary artery. In brief, a thoracotomy was performed via the fourth intercostal space, the heart was exposed, and ECG was then monitored. An 8-0 polypropylene suture was passed loosely around the left anterior descending (LAD) coronary artery near its origin. Once hemodynamics were stabilized, LAD occlusion was performed by tightening the suture loop. Acute myocardial ischemia was deemed successful on the basis of elevation of the ST segment on ECG. After 1 hr, mice with MI were randomly divided into two groups and were injected with 20 μl of virus solution (2×10^9 plaque-forming units/ml in PBS) of Ad.Null ($n=12$) or Ad.hTK ($n=12$) into the peri-infarct zone. Expression and localization of hTK in left ventricles after gene delivery were identified at 3 and 7 days after gene delivery by immunohistochemical staining; normal rabbit IgG was substituted for primary antibodies as negative control. Human kallikrein levels in mouse serum were determined at 3 and 7 days post gene delivery using an enzyme-linked immunosorbent assay (ELISA) specific for hTK.

Functional assessment

Under mild isoflurane anesthesia, echocardiography was performed to obtain a baseline examination prior to the operation, 7 days after MI, using a Vevo 770 echocardiography system (VisualSonics, Toronto, ON, Canada) with a 12-MHz transducer. Left ventricular end-diastolic volume (LVEDV), left ventricular end-systolic volume (LVESV), left ventricular end-diastolic diameter (LVEDD), and left ventricular end-systolic diameter (LVESD) were measured. Left ventricular ejection fraction (EF) and left ventricular fractional shortening (FS) were calculated with standard M-mode echocardiographic equations (EF = LVEDV − LVESV/LVEDV × 100; FS = LVEDD − LVESD/LVEDD × 100). All measurements were averaged for five consecutive cardiac cycles and performed by an experienced examiner in a blinded fashion.

Quantification of circulating EPCs

For quantification of peripheral circulating EPCs by flow cytometry, blood was withdrawn via intracardiac puncture ($n=5$ mice per group) at 7 days post MI. Mononuclear cells were isolated from 1 ml of peripheral blood by density gradient centrifugation using Histopaque-1077 solution. One-half of the PBMCs were incubated for 30 min on ice with FITC-conjugated anti-mouse CD34 and phycoerythrin (PE)-conjugated anti-mouse Flk-1 (BD Biosciences). After incubation, cells were washed with PBS. Data were acquired using a FACScan cytometer equipped with a 488-nm argon laser and a 620-nm red diode laser and analyzed using CellQuest software (Becton Dickinson). For quantification of EPCs, the number of $CD34^+$ $Flk\text{-}1^+$ cells within the monocytic cell population was counted.

Circulating EPC numbers were also determined by colony-forming unit (CFU) assay. The other one-half of PBMCs were plated on fibronectin-coated 24-well plates in EGM-2. To exclude mature endothelial cells, nonadherent cells were collected after 48 hr and plated in replicate on fibronectin-coated 24-well plates. Colonies were quantified at day 7. A colony was defined as a central core of "round" cells with more elongated "sprouting" cells at the periphery, and is referred to as early outgrowth CFU-endothelial cells (CUF-ECs) (Hill *et al*., 2003).

Quantification of EPCs in the heart

For quantification of EPCs in infarcted hearts of Ad.Null- or Ad.hTK-treated mice at 3 days after MI by flow cytometry, hearts were collected, and the right ventricular free wall was excised. The remainder of the heart was triturated in PBS supplemented with 2% fetal bovine serum (FBS) on ice with a Medimachine (BD Biosciences) and filtered through a 70-μm nylon mesh (BD Biosciences). Single-cell suspensions were centrifuged, resuspended in PBS with 2% FBS, and incubated with antibody for 30 min on ice. After washing, immunofluorescence was detected by flow cytometry. Flow-cytometric identification of the cells was performed through simultaneous labeling with PE-conjugated anti-mouse Flk-1 and FITC-conjugated anti-mouse CD34 (BD Biosciences).

Histological analysis

After the echocardiographic image acquisition at 7 days post MI, mice were anesthetized with sodium pentobarbital (50 mg/kg, i.p.). The heart was rapidly excised after PBS perfusion. Cardiac tissues were fixed with 4% paraformaldehyde and embedded. Four-micrometer sections were obtained for morphological analyses. Sections were subjected to Masson's trichrome staining or immunohistochemical analysis using a staining kit (Vector Laboratories, Burlingame, CA) according to the manufacturer's instructions. Angiogenesis was quantitatively assessed by $CD31^+$ staining for determination of capillary density, and α-smooth muscle actin (α-SMA)–positive staining for determination of arteriolar density. Capillaries were identified as having a diameter $<20\,\mu$m and a layer of endothelial cells without smooth muscle cells, whereas arterioles were identified as having a diameter $>20\,\mu$m and $<100\,\mu$m with a layer of smooth muscle cells. To determine capillary density and arteriole density, the number of positive staining was counted in a double-blind fashion from 10 different fields of each section in the peri-infarct zone ($n=5$). The average number of vessels

in one section was used for assessment of vascular density. Primary antibody against CD68 (clone FA-11; BioLegend, San Diego, CA) was used for immunostaining of macrophages. The number of $CD68^+$ cells was counted in a double-blind fashion from 10 different fields of each section ($n=5$) at $400\times$ magnification.

Identification of EPCs within the infarct border zone of MI was evaluated using confocal laser scanning microscopy. Sections were also incubated with a combination of the primary antibodies rat anti-mouse Flk-1 (1:50 dilution) and FITC-conjugated anti-mouse CD34 (BD Biosciences), to confirm bone marrow-derived cells in the infarct area.

Statistical analysis

Data were compared among experimental groups using ANOVA followed by Fisher's PLSD. Data were expressed as means ± SEM. Differences were considered statistically significant at a value of $p<0.05$.

Results

TK increases EPC differentiation

PBMCs were isolated by density gradient centrifugation and differentiated into EPCs after 7 days of culture. EPCs were characterized by assessing FITC-conjugated UEA-1-lectin binding (green) and Dil-Ac-LDL uptake (red) (Fig. 1A). EPCs were positive for kinin B_2R staining (Fig. 1B). Compared with the control group (11.5 ± 0.6%), the percentage of double-positive Dil-Ac-LDL/UEA-1-lectin cells was increased after treatment with TK and BK after 7 days in culture (22.6 ± 1.1% and 21.3 ± 1.1%, respectively; $p<0.01$ vs. control), indicating that TK and BK stimulated the differentiation of cultured EPCs expanded from PBMCs (Fig. 1C and D).

FACS-computed counting (Fig. 1E and F) of EPC positive for Dil-LDL/lectin dual staining revealed that 7 days with BK and TK determined a consistent increase of EPC number compared with control cells ($p<0.01$ vs. control).

Cultured cells at passage 3 were positive for the endothelial lineage markers KDR and CD31, and stained positive for progenitor cell marker CD34, although most cells did not express the hematopoietic lineage marker CD45 (Fig. 1G). These cells were identified as EPCs.

TK improves migration of EPCs and formation of tube-like structures on Matrigel

The effect of TK on EPC migration was analyzed in a modified Boyden chamber assay. Ad.hTK increased EPC migration by profoundly enhancing cell migration compared with Ad.Null (4.2 ± 0.8% vs. 1.3 ± 0.3%; $p<0.01$). Cotreatment with icatibant and LY294002 significantly blocked TK's effect (2.1 ± 0.4% and 1.3 ± 0.1%, respectively; $p<0.01$ vs. TK) (Fig. 1H and J).

To study the effect of TK on the contribution of EPCs to tube formation, quantification of the length of tube showed that EPCs treated with Ad.hTK had 1.58-fold higher tubes as compared with control EPCs ($p<0.01$). Cotreatment with icatibant and LY294002 significantly blocked TK's effect (1.0 ± 0.1 and 0.98 ± 0.1, respectively; $p<0.01$ vs. TK) (Fig. 1I and K).

TK reduces hypoxia-induced apoptosis of EPCs

The EPC apoptosis rate was detected by flow cytometry. The apoptosis rate of EPCs significantly increased after 12 hr under hypoxic conditions (54.8 ± 6.7%), whereas TK treatment protected EPCs from hypoxia-induced apoptosis (20.8 ± 4.4%; $p<0.01$). Cotreatment with icatibant and LY294002 significantly blocked TK's effect (36.6 ± 4.7% and 55.8 ± 6.3%, respectively; $p<0.01$ vs. hypoxia/TK) (Fig. 2A and B).

We further investigated the effect of TK on the Akt signaling pathway in EPCs. Figure 2C shows that transduction of Ad.hTK in hypoxia-injured EPCs resulted in increased phosphorylation of Akt and reduced cleaved caspase-3 levels. However, these effects were blocked by icatibant and LY294002 (Fig. 2C). Expression of hTK in EPCs after Ad.hTK transduction was confirmed by immunocytochemistry (Fig. 2D).

Myocardial expression of hTK after gene delivery

Using intramyocardial injection strategy, we delivered Ad.hTK locally into the mouse left ventricle. Expression and localization of recombinant hTK were identified immunohistochemically in the left ventricle at 3 and 7 days after gene delivery. Immunohistochemistry showed expression of hTK in mouse cardiomyocytes (Fig. 3A). No specific staining was found in the left ventricle injected with control adenovirus Ad.Null. hTK was detected in mouse serum at 3 and 7 days post gene delivery (369 ± 76 and 122 ± 47 ng/ml, respectively; $n=5$) by ELISA. Human kallikrein was not detectable in mice injected with control virus. These results demonstrate that hTK was expressed in mouse heart after local gene delivery.

TK increases cardiac function after MI

Seven days after intramyocardial injection, TK significantly reduced infarct size in the left ventricle compared with the MI/Ad.Null control group, as determined by Masson's

FIG. 1. Characterization of cultured PBMCs and the effect of TK on EPC function. **(A)** At day 7 after PBMC isolation, adherent cells intensively took up Dil-Ac-LDL and bound an endothelial-specific lectin-FITC as revealed by fluorescence microscopy. **(B)** Positive staining for kinin B_2R in the cultured EPCs. **(C)** TK and BK stimulated differentiation of cultured EPCs expanded from PBMCs. **(D)** Quantitative analysis of the percentage of cells positive for Dil-LDL/lectin dual staining. **(E)** Representative FACS data. **(F)** Quantitative fluorescence analysis was determined by FACS-computed counting. **(G)** EPCs are identified by culture of PBMCs. EPCs were positive for the endothelial lineage markers KDR and CD31 and stained positive for progenitor cell marker CD34, but most cells did not express the hematopoietic lineage marker CD45. **(H)** Migration was evaluated using Transwell apparatus. TK profoundly enhanced cell migration compared with control. EPC migration was inhibited by cotreatment with the B_2R antagonist icatibant and the PI3K inhibitor LY294002. **(I)** Tube formation of EPCs stimulated by TK was inhibited by cotreatment with icatibant and LY294002. **(J)** Migrating cells are presented as the percentage of seeded EPCs. *$p<0.05$ vs. other groups. **(K)** Quantitative analysis of the mean tube length was measured using Image-Pro Plus and was calculated against control groups. *$p<0.05$ vs. other groups. Original magnification: $200\times$.

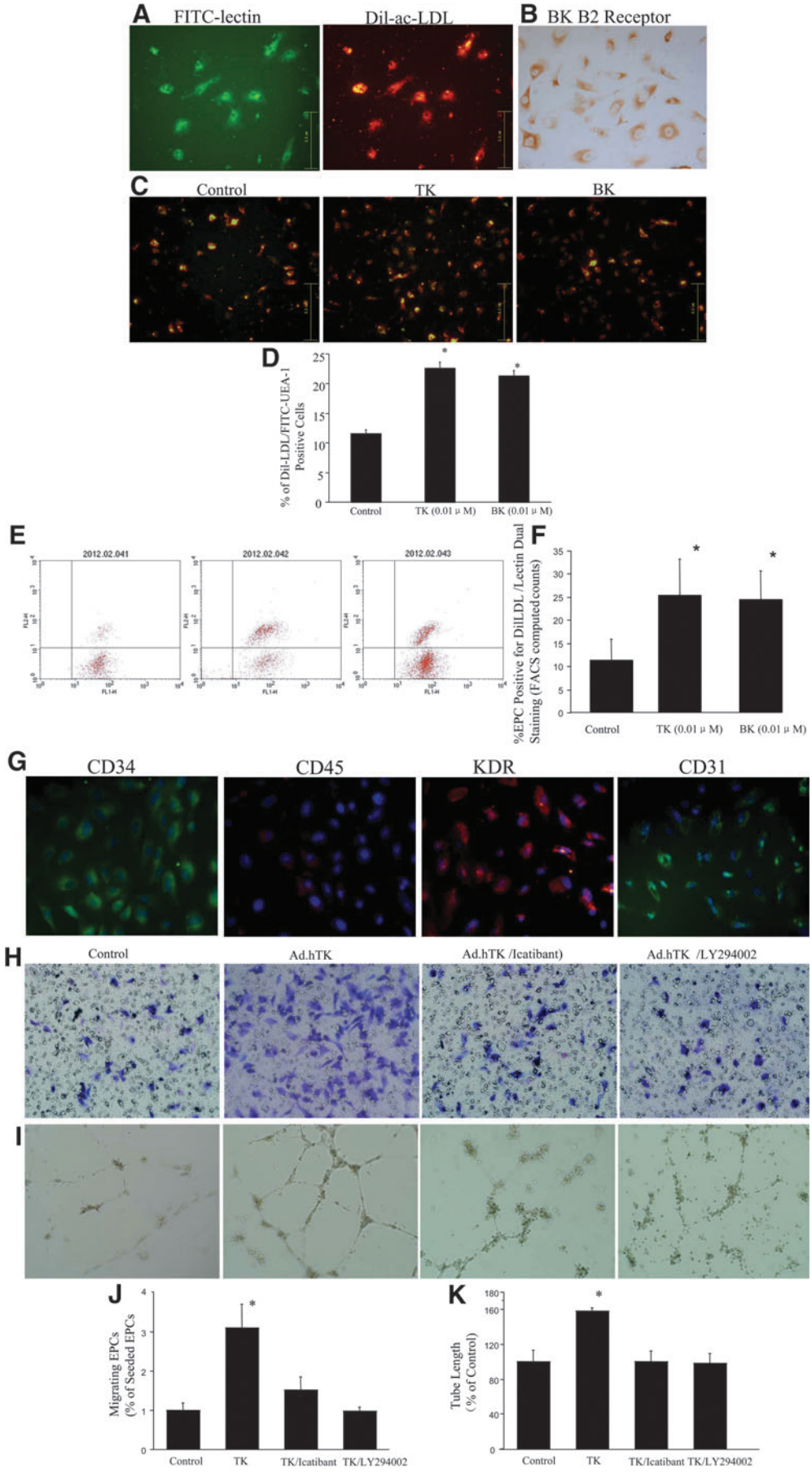
A
FITC-lectin
Dil-ac-LDL
B
BK B2 Receptor
C
Control
TK
BK
D
% of Dil-LDL/FITC-UEA-1 Positive Cells
Control
TK (0.01 μ M)
BK (0.01 μ M)
E
2012.02.041
2012.02.042
2012.02.043
F
%EPC Positive for DilLDL /Lectin Dual Staining (FACS computed counts)
Control
TK (0.01 μ M)
BK (0.01 μ M)
G
CD34
CD45
KDR
CD31
H
Control
Ad.hTK
Ad.hTK /Icatibant)
Ad.hTK /LY294002
I
J
Migrating EPCs (% of Seeded EPCs
Control
TK
TK/Icatibant
TK/LY294002
K
Tube Length (% of Control)
Control
TK
TK/Icatibant
TK/LY294002

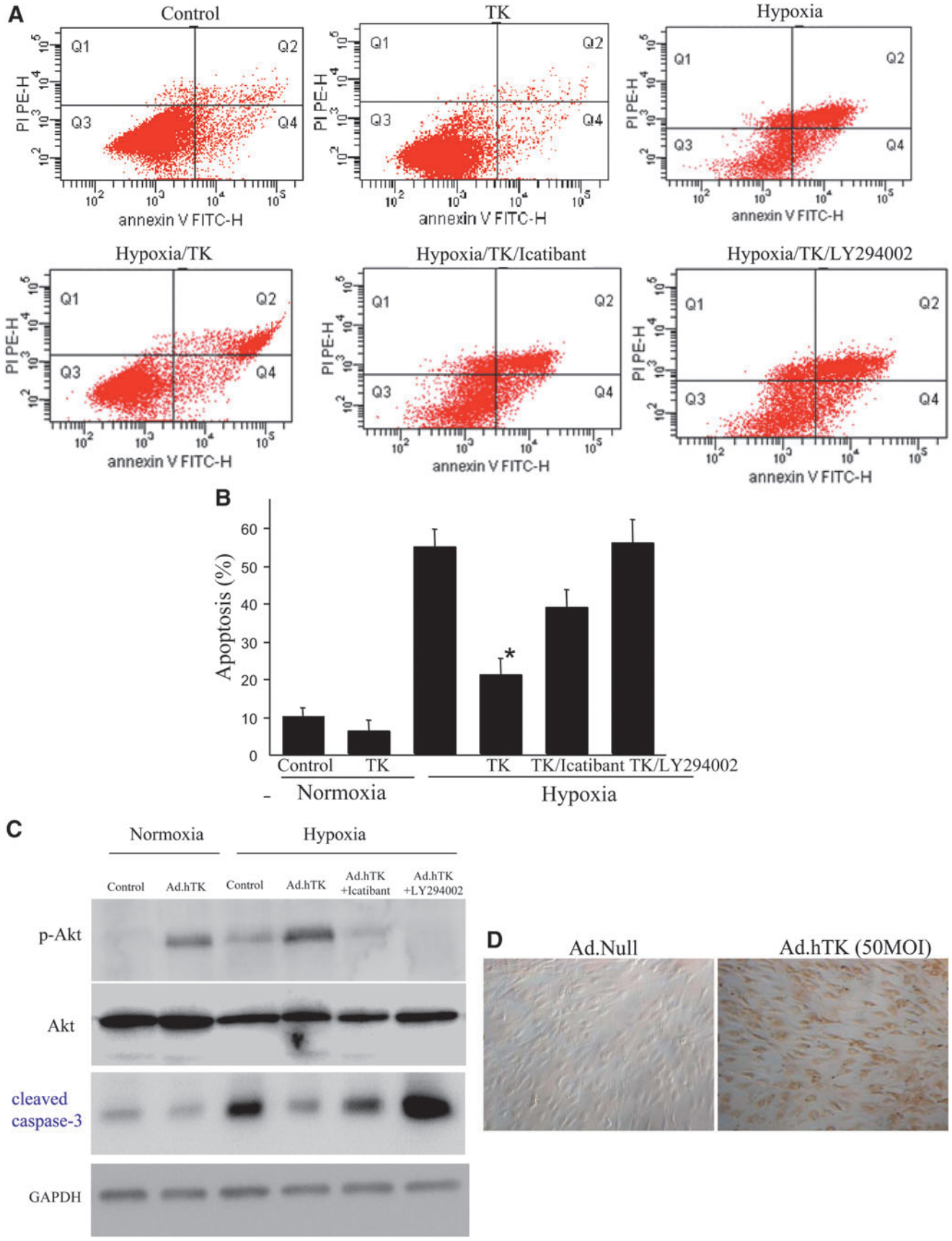

FIG. 2. TK reduced EPC apoptosis induced by hypoxia. **(A)** Representative flow-cytometric analysis of apoptosis shows that TK treatment protects EPCs from hypoxia-induced apoptosis. Cotreatment with icatibant and LY294002 significantly blocked TK's effect. **(B)** Quantitative analysis of EPC apoptosis by flow cytometry. $^*p < 0.05$ vs. other groups. **(C)** Western blots for Akt and cleaved caspase-3. **(D)** Expression of hTK in EPCs after Ad.hTK transduction was confirmed by immunocytochemistry. Original magnification: 200×.

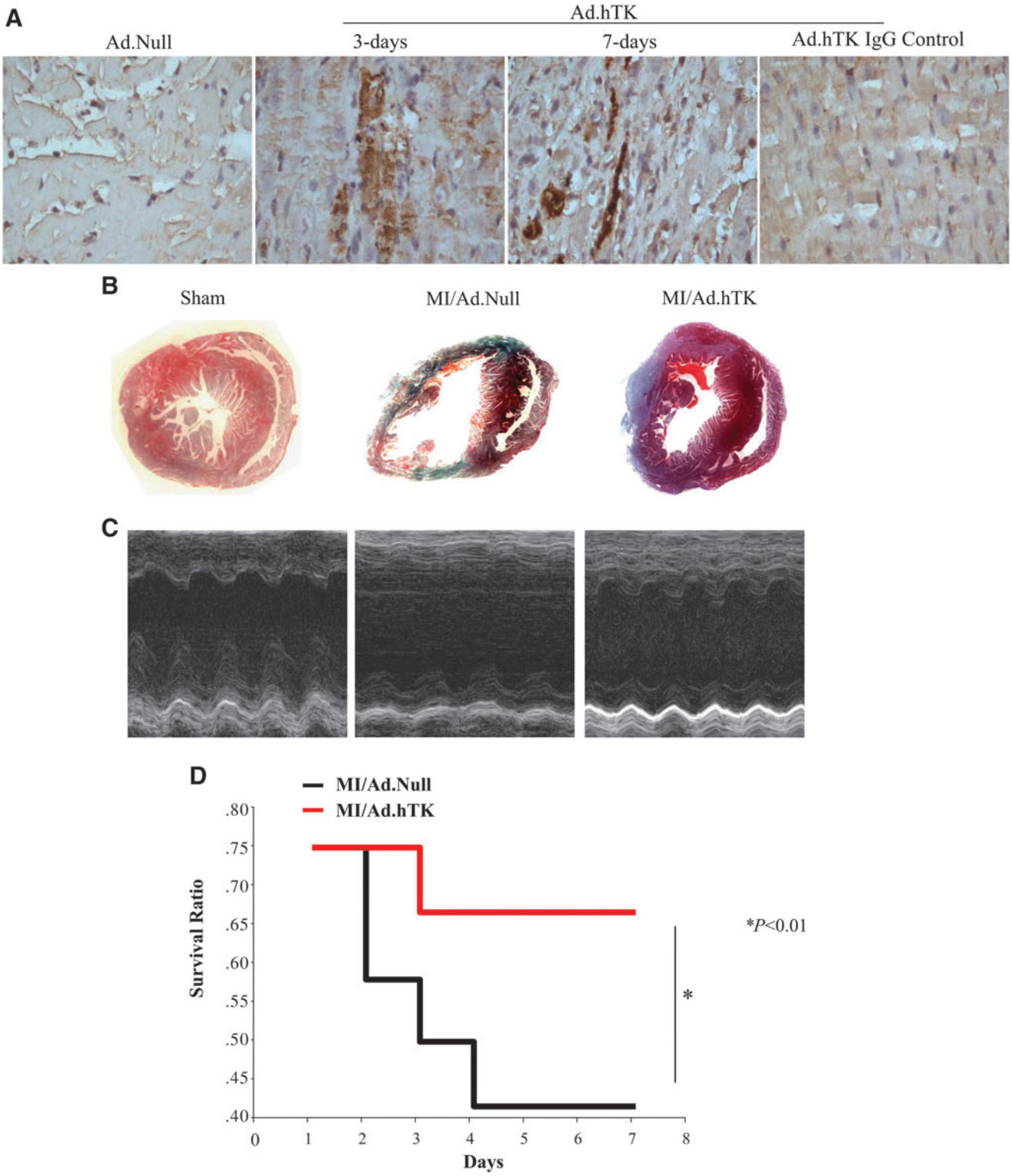

FIG. 3. TK gene therapy increases survival rate and reduces infarct size. **(A)** Representative immunohistochemistry photographs of transgenic hTK protein expression in the infarcted region of mouse hearts at 3 and 7 days after MI. A variable amount of immunoreactive hTK is observed in Ad.hTK-injected groups. Rabbit IgG was substituted for primary antibodies as negative control. Original magnification: 200×. **(B)** Representative Masson's trichrome staining. Original magnification: 10×. Significantly reduced scar area in the Ad.hTK-treated hearts was observed 7 days after MI compared with the Ad.Null group. **(C)** Representative M-mode images at the level of papillary muscles. **(D)** A survival analysis was performed for the Ad.Null- ($n=12$) and Ad.hTK-treated ($n=12$) mice after MI. TK treatment increased survival rate compared with the Ad.Null group 7 days after MI. *$p<0.01$ vs. MI/Ad.Null.

Table 1. Effects of Kallikrein on Cardiac Function 7 Days After MI

Variable	*Baseline*	*Sham*	*MI/Ad.Null*	*MI/Ad.hTK*
Infarct size (%)	0	0	39.5 ± 9.1	17.9 ± 6.1[a]
HW/BW (mg/g)	4.5 ± 0.1	4.9 ± 0.9	6.6 ± 0.3	5.7 ± 0.5[a]
EF (mmHg)	65.2 ± 2.3	62.7 ± 3.6	24.6 ± 4.9	38 ± 6.9[a]
FS (mmHg)	33.6 ± 2.1	32.8 ± 2.6	11.4 ± 2.5	18.2 ± 3.2[a]
LVIDD (mmHg/sec)	3.0 ± 0.2	3.1 ± 0.2	5.1 ± 0.4	4.4 ± 0.5[a]
LVIDS (mmHg/sec)	2.0 ± 0.2	2.1 ± 0.1	4.5 ± 0.4	3.5 ± 0.4[a]

BW, body weight; EF, ejection fraction; FS, fractional shortening; HW, heart weight; LVIDD, left ventricular inner diastolic diameter; LVIDS, left ventricular inner systolic diameter; MI, myocardial infarction.

Values are means ± SEM. $n = 5$ in each group.

[a]$p < 0.05$ vs. Baseline, Sham, and MI/Ad.Null.

trichrome staining and quantitative analysis (Fig. 3B and Table 1). Transthoracic echocardiographic examination was performed to evaluate cardiac function after MI. The EF was markedly reduced after MI, but was partially restored by hTK gene delivery (Fig. 3C and Table 1). Characteristic impairments in contractility (left ventricular inner systolic diameter) and diastolic function (left ventricular inner diastolic diameter) after MI were significantly improved after TK injection (Table 1). Heart weight/body weight ratios were increased 7 days after MI, but were reduced by hTK gene therapy (Table 1). Furthermore, we observed that treatment with TK significantly decreased MI-related mortality. As shown in Fig. 3D, 67% of MI/Ad.hTK mice, but only 42% of MI/Ad.Null mice, survived ($p < 0.01$) 7 days after the induction of MI.

TK administration increases the number of CD34$^+$ Flk-1$^+$ progenitors in blood and heart

To evaluate the potential EPC-mobilizing activity of TK gene transfer 7 days after MI, we analyzed EPC-like PBMCs by flow cytometry. EPC-like PBMCs were identified by positive staining for CD34 and Flk-1. The numbers of CD34$^+$Flk-1$^+$ cells in peripheral blood were significantly increased in MI/Ad.hTK mice compared with MI/Ad.Null control mice (Fig. 4A and B). We further identified the formation of EPC colonies by CFU-EC assay (Fig. 4C). The number of murine CFU-ECs was significantly increased in the MI/Ad.hTK group compared with the MI/Ad.Null group (4.4 ± 0.9 vs. 1.8 ± 0.8; $p < 0.05$). TK induced a significant mobilization of EPCs in the peripheral circulation. Dil-Ac-LDL uptake and lectin binding confirmed that the CFU-ECs differentiate to the EC lineage.

We also measured the percentage of CD34$^+$FLK-1$^+$ cells in the infarcted myocardial tissue. Flow-cytometry analysis showed that TK gene transfer caused significantly increased CD34$^+$Flk-1$^+$ cells compared with Null treatment mice (3.37 ± 0.5 vs. 0.63 ± 0.5, respectively; $p < 0.05$; Fig. 4E and F). As shown in Fig. 4G, CD34$^+$Flk-1$^+$ cells were also identified in the peri-infarct border zone, and double-staining cells formed capillary-like structures in the Ad.hTK-injected heart. Our results show that TK gene delivery promotes the recruitment of CD34$^+$Flk-1$^+$ bone marrow–derived cells into the vascular wall.

TK attenuates intramyocardial inflammation

Inflammatory cell accumulation in the infarcted region of the heart was identified by CD68 immunostaining (Fig. 5A). CD68$^+$ cells were counted for quantification of macrophage number (Fig. 5B). Increased macrophage cell infiltration was detected in the infarct area of the heart after MI, but kallikrein significantly decreased CD68$^+$ cells compared with the control.

TK increases peri-infarct angiogenesis and arteriogenesis

At 7 days post MI, marked angiogenesis was observed in the area between necrosis tissue and surviving myocardium. Capillary density in the peri-infarct area was determined by immunohistochemical staining of CD31 (Fig. 5C). Quantitative analysis indicated that the capillary density was significantly increased in the MI/Ad.hTK group compared with the MI/Ad.Null group (197 ± 10 vs. 100 ± 16 capillaries/mm^2; $p < 0.05$) (Fig. 5E); in the sham group, the capillary density was 1,930.5 ± 117/mm^2. Moreover, small-sized arterioles were clearly visible in the tissue sections stained with an antibody against α-SMA (Fig. 5D), and quantitative analysis indicated that arteriole density was significantly increased in the TK treatment group compared with the MI/Ad.Null group (111.6 ± 24.0 vs. 50.8 ± 7.0; $p < 0.05$) (Fig. 5F); arteriole density in the sham was 76.1 ± 6.1/mm^2.

Discussion

After severe ischemia, restoration of the blood supply to the border area can prevent progressive cardiomyocyte death and cardiac remodeling, thus improving cardiac function and mortality. Therefore, therapeutic angiogenesis has become a promising new method of treatment for patients with ischemic heart disease. Several strategies have been developed to promote vascular growth, including growth factor delivery (Yancopoulos *et al.*, 2000), cell-based therapy, and gene therapy. Studies in animals and humans suggest that EPCs ameliorate the function of ischemic organs possibly by both induction of vasculogenesis and angiogenesis. A critical limitation, so far, for the therapeutic application of postnatal EPCs is their low number in the circulation, which is further reduced in patients with cardiovascular risk factors (Vasa *et al.*, 2001). Consequently, understanding the regulation of EPCs and their mechanisms may provide new insights into therapeutic neovascularization.

Our group and others have investigated the beneficial effects of the KKS on neovascularization after ischemia (Emanueli *et al.*, 2000; Yao *et al.*, 2007; Stone *et al.*, 2009). A recent publication demonstrated that hTK is crucial for proangiogenic cell invasiveness and activity by both protease- and

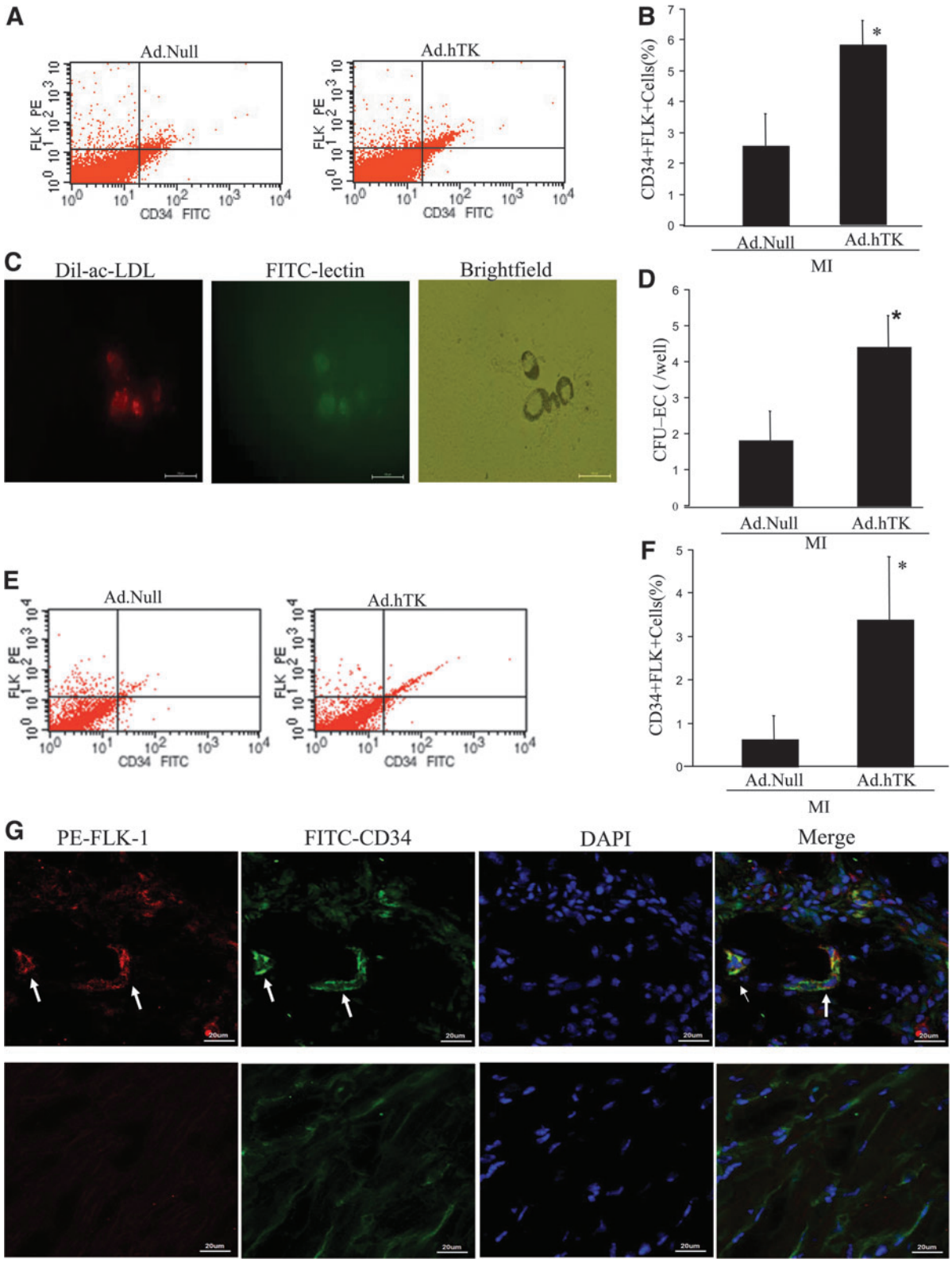

FIG. 4. TK administration increases the number of $CD34^+Flk\text{-}1^+$ progenitors in mice. **(A)** Representative FACS data, in which the $CD34^+Flk\text{-}1^+$ cells within the monocytic cell population of the blood were judged as EPCs. **(B)** Quantitative evaluation of EPCs by FACS analysis. **(C)** The effect of TK on CFU-EC numbers. After 7 days in culture, EPCs were double-stained with Dil-Ac-LDL and FITC-conjugated UEA lectin, and analyzed by fluorescent microscopy. **(D)** Quantitative evaluation of CFUs. **(E)** Representative FACS data, in which the $CD34^+Flk\text{-}1^+$ cells within heart tissue were judged as EPCs. **(F)** Relative percentage of $CD34^+Flk\text{-}1^+$ EPCs in heart tissues post MI. $^*p < 0.05$. **(G)** EPCs were identified in the peri-infarction zone. Immunofluorescent staining using CD34 (green) and Flk-1 (red) antibodies identified $CD34^+Flk\text{-}1^+$ cells. Nuclei were counterstained with DAPI (blue). Upper panels show representative photomicrographs of cross sections of Ad.hTK-injected heart; white arrows show positive staining. Lower panels show representative photomicrographs of cross sections of Ad.Null-injected heart. Original magnification: 800×. $^*p < 0.05$ vs. MI/Ad.Null; $n = 5$.

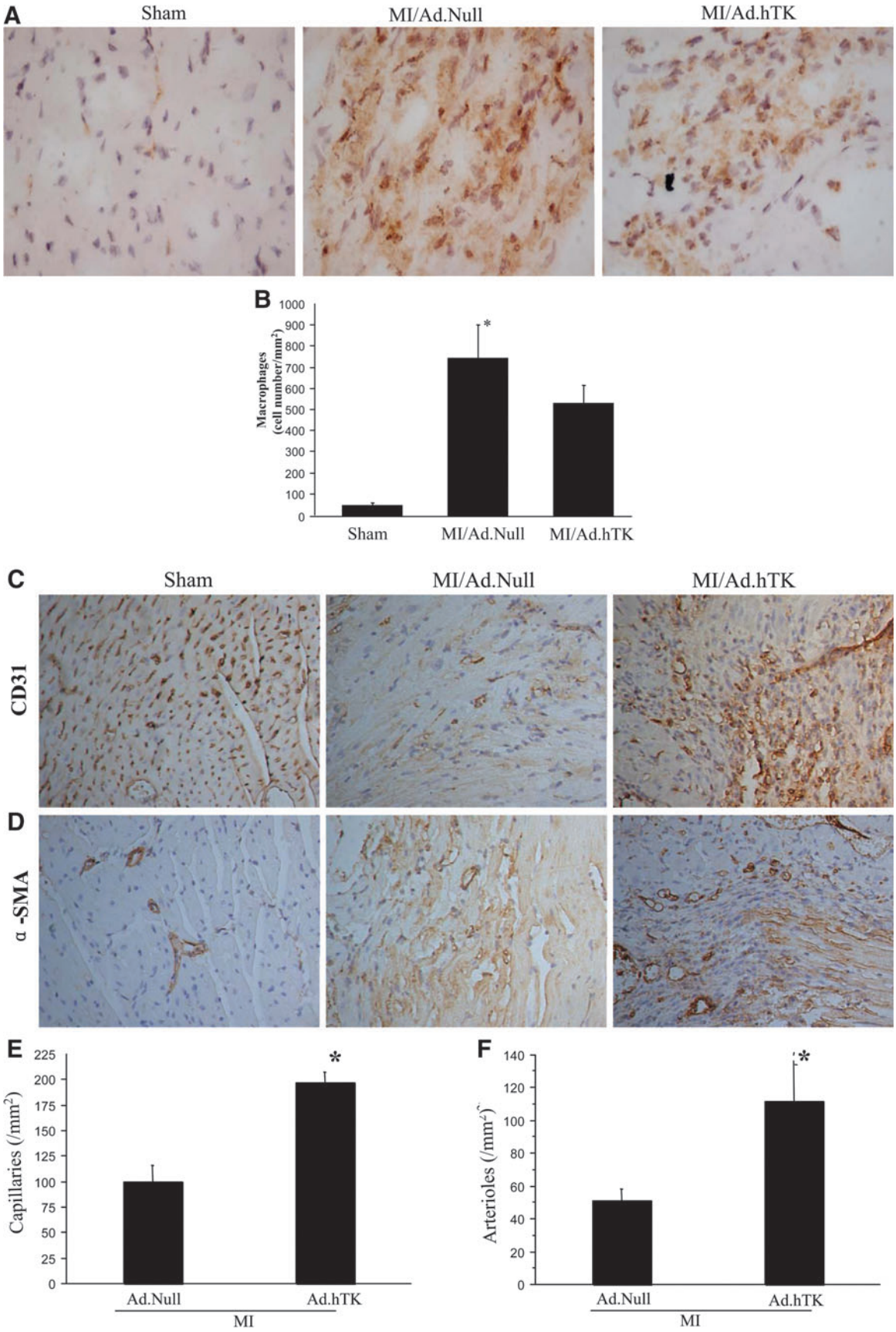

FIG. 5. Effects of hTK on the number of macrophages, capillary density, and arteriole density 7 days after MI. **(A)** Representative images of CD68 immunostaining in the infarcted area. Original magnification: 400×. **(B)** Quantitative analysis of $CD68^+$ cells. Representative photographs of immunostaining using **(C)** CD31 to identify capillaries and **(D)** αα-SMA to identify arterioles are shown. Original magnification: 200×. Quantitative analysis of **(E)** capillary density and **(F)** arteriole density in the peri-infarct myocardium is also shown. *$p < 0.05$ vs. MI/Ad.Null; $n = 5$.

kinin receptor–mediated mechanisms (Spinetti *et al*., 2011). The direct effects of TK on differentiation of PBMCs into EPCs and their angiogenic properties are not known. In the present study, we explored the mechanisms by which TK exerted positive effects on EPC function. TK treatment enhanced the differentiation of rat PBMCs into EPCs during culture for 7 days. TK, via B_2R-Akt activation, improved EPC differentiation, migration, and tube formation capacity. We demonstrated that the kinin B_2R mediates TK's actions on EPCs, as icatibant abolished the effects of TK. Furthermore, Akt may constitute a key signaling pathway in the angiogenic activity of early EPCs (Thum *et al*., 2007). Previous studies showed that TK stimulates the activation of Akt *in vitro* and *in vivo* (Kränkel *et al*., 2008; Yao *et al*., 2008). In this study, the PI3K inhibitor LY294002 abolished TK-induced EPC migration and tube formation, indicating that TK regulates EPC function by a mechanism dependent on PI3K activity.

We found that EPCs treated with TK showed a greater resistance to hypoxia-mediated cellular apoptosis, in conjunction with increased Akt phosphorylation and decreased cleaved caspase-3 protein levels. A previous study showed that kallikrein/kinin inhibits GSK-3β and caspase-3 activity by Akt activation in the ischemic myocardium (Yin *et al*., 2005). Taken together, these findings suggest that the KKS may protect against hypoxia-induced apoptosis of EPCs by activating the PI3K-Akt pathway. Increased survival of implanted stem cells is essential to stem-cell therapy. Indeed, it has been shown that more than 99% of mesenchymal stem cells die 4 days after transplantation into uninjured left ventricles of nude mice (Toma *et al*., 2002). Our results demonstrate that TK protects EPCs from hypoxia-induced apoptosis, indicating a promising strategy to increase the efficacy of stem-cell therapy.

Adenovirus-mediated hTK gene transfer was previously found to increase the number of circulating EPCs (Spillmann *et al*., 2006). In our study, we used two different methods to evaluate the effect of TK on circulating EPC numbers. One used flow cytometry for assessment of circulating cells positive for CD34 and Flk-1 (Heeschen *et al*., 2003), and the other method used the CFU assay (George *et al*., 2004). Of the two methods, $CD34^+Flk\text{-}1^+$ staining is more appropriate for defining circulating EPCs, whereas CFU numbers are more likely to reflect their ability to proliferate (George *et al*., 2006). Our data demonstrate an enhancement of peripheral EPCs in mice with TK gene transfer after MI. Otherwise, we were able to analyze the presence of $CD34^+Flk\text{-}1^+$ EPCs using flow cytometry, especially in the infarct myocardium. These results further confirmed that the increased circulating CD34/Flk cells can home to the infarcted myocardial tissue after TK gene therapy, and these cells contributed to increased neovascularization. However, it is still unknown as to the exact mechanism by which TK increases the number of circulating EPCs. Possibly, Ad.hTK gene transfer can up-regulate circulating TK and BK levels, which reach the bone marrow and stimulate the release of EPCs through endothelial nitric oxide synthase and matrix metalloproteinase-dependent pathways (Heeschen *et al*., 2003; Kränkel *et al*., 2008).

In this study, we observed that hTK gene transfer significantly improved short-term survival and functional outcome at 7 days after MI. Previously, it was shown that adenovirus-mediated gene transfer of hTK reduced the stroke-induced mortality rate in Dahl salt-sensitive rats (Zhang *et al*., 1999). The cardioprotective role of the KKS has been well documented in the setting of acute myocardial ischemia (Griol-Charhbili *et al*., 2005). Pons and colleagues examined the long-term effects of TK deficiency on survival and left ventricular remodeling after MI, as $TK^{-/-}$ mice displayed an increased mortality rate and aggravation of left ventricular hypertrophy and dilatation in comparison with $TK^{+/+}$ (Pons *et al*., 2008). The mechanisms whereby kallikrein gene transfer results in attenuation of the mortality rate in MI mice is probably related to inhibition of cardiomyocyte apoptosis and promotion of neovascularization, thereby restoring regional blood flow and improving cardiac function (Yin *et al*., 2005; Yao *et al*., 2007). Prevention of apoptosis and the provision of sufficient tissue oxygenation are the possible mechanisms of TK's cardioprotective effects. Recently, results consistently demonstrated that kallikrein overexpression stimulates a well-organized and functional neovascularization, as the KKS can increase circulating proangiogenic cells' invasive and proangiogenic activities, which may play a role in multiple steps of postnatal vasculogenesis (Stone *et al*., 2009; Spinetti *et al*., 2011). Our results confirmed that overexpression of TK promotes neovascularization by maximization of EPC number and function via activation of the PI3K-Akt pathway. The exact mechanism underlying the effect of KKS on EPC function is not entirely understood and deserves further attention.

Taken together, the present study demonstrates that TK promotes vessel growth after MI by increasing the number of circulating EPCs and enhancing EPC differentiation, migration, tube-formation capacity, and survival through a kinin B_2R-dependent Akt signaling pathway. Therefore, augmentation and enhancement of circulating EPC numbers and activity by TK might be a novel strategy to improve neovascularization after tissue ischemia.

Acknowledgments

We would like to acknowledge grant support for our laboratory from National Natural Science Foundation of China (30871071, 81070085 to Yuyu Yao).

Author Disclosure Statement

The authors state no conflict of interest.

References

Chavakis, E,, Urbich, C., and Dimmeler, S. (2008). Homing and engraftment of progenitor cells: a prerequisite for cell therapy. J. Mol. Cell. Cardiol. 45, 514–522.

Ebrahimian, T.G., Heymes, C., You, D., *et al*. (2006). NADPH oxidase-derived overproduction of reactive oxygen species impairs postischemic neovascularization in mice with type 1 diabetes. Am. J. Pathol. 169, 719–728.

Emanueli, C., Zacheo, A., Minasi, A., *et al*. (2000). Adenovirus-mediated human tissue kallikrein gene delivery induces angiogenesis in normoperfused skeletal muscle. Arterioscler. Thromb. Vasc. Biol. 20, 2379–2385.

George, J., Goldstein, E., Abashidze, S., *et al*. (2004). Circulating endothelial progenitor cells in patients with unstable angina: association with systemic inflammation. Eur. Heart J. 12, 1003–1008.

George, J., Shmilovich, H., Deutsch, V., *et al*. (2006). Comparative analysis of methods for assessment of circulating endothelial progenitor cells. Tissue Eng. 12, 331–335.

Griol-Charhbili, V., Messadi-Laribi, E., Bascands, J.L., *et al*. (2005). Role of tissue kallikrein in the cardioprotective effects of ischemic and pharmacological preconditioning in myocardial ischemia. FASEB J. 19, 1172–1174.

Heeschen, C., Aicher, A., Lehmann, R., *et al*. (2003). Erythropoietin is a potent physiologic stimulus for endothelial progenitor cell mobilization. Blood 102, 1340–1346.

Hill, J.M., Zalos, G., Halcox, J.P.J., *et al*. (2003). Circulating endothelial progenitor cells, vascular function, and cardiovascular risk. N. Engl. J. Med. 348, 593–600.

Isner, J.M., and Asahara, T. (1999). Angiogenesis and vasculogenesis as therapeutic strategies for postnatal neovascularization. J. Clin. Invest.103, 1231–1236.

Kawamoto, A., Gwon, H.C., Iwaguro, H., *et al*. (2001). Therapeutic potential of ex vivo expanded endothelial progenitor cells for myocardial ischemia. Circulation 103, 634–637.

Kocher, A.A., Schuster, M.D., Szabolcs, M.J., *et al*. (2001). Neovascularization of ischemic myocardium by human bone-marrow-derived angioblasts prevents cardiomyocyte apoptosis, reduces remodeling and improves cardiac function. Nat. Med. 7, 430–436.

Kränkel, N., Katare, R.G., Siragusa, M., *et al*. (2008). Role of kinin B_2 receptor signaling in the recruitment of circulating progenitor cells with neovascularization potential. Circ. Res. 103, 1335–1343.

Loomans, C.J., de Koning, E.J., Staal, F.J., *et al*. (2004). Endothelial progenitor cell dysfunction: a novel concept in the pathogenesis of vascular complications of type 1 diabetes. Diabetes 53, 195–199.

Madeddu, P., Emanueli, C., and El-Dahr, S. (2007). Mechanisms of disease: the tissue kallikrein-kinin system in hypertension and vascular remodeling. Nat. Clin. Pract. Nephrol. 3, 208–221.

Pons, S., Griol-Charhbili, V., Heymes, C., *et al*. (2008). Tissue kallikrein deficiency aggravates cardiac remodelling and decreases survival after myocardial infarction in mice. Eur. J. Heart Fail. 10, 343–351.

Serhan, C.N., Fierro, I.M., Chiang, N., and Pouliot, M. (2001). Cutting edge: nociceptin stimulates neutrophil chemotaxis and recruitment: inhibition by aspirin-triggered-15-epi-lipoxin A_4. J. Immunol. 166, 3650–3654.

Silva, J.-A., Jr., Araujo, R.C., Baltatu, O., *et al*. (2000). Reduced cardiac hypertrophy and altered blood pressure control in transgenic rats with the human tissue kallikrein gene. FASEB J. 14, 1858–1860.

Spillmann, F., Graiani, G., Van Linthout, S., *et al*. (2006). Regional and global protective effects of tissue kallikrein gene delivery to the peri-infarct myocardium. Regen. Med. 1, 235–254.

Spinetti, G., Fortunato, O., Cordella, D., *et al*. (2011). Tissue kallikrein is essential for invasive capacity of circulating proangiogenic cells. Circ. Res.108, 284–293.

Stone, O.A., Richer, C., Emanueli, C., *et al*. (2009). Critical role of tissue kallikrein in vessel formation and maturation: implications for therapeutic revascularization. Arterioscler. Thromb. Vasc. Biol. 29, 657–664.

Thum, T., Fraccarollo, D., Schultheiss, M., *et al*. (2007). Endothelial nitric oxide synthase uncoupling impairs endothelial progenitor cell mobilization and function in diabetes. Diabetes 56, 666–674.

Toma, C., Pittenger, M.F., Cahill, K.S., *et al*. (2002). Human mesenchymal stem cells differentiate to a cardiomyocyte phenotype in the adult murine heart. Circulation 105, 93–98.

Vasa, M., Fichtlscherer, S., Aicher, A., *et al*. (2001). Number and migratory activity of circulating endothelial progenitor cells inversely correlate with risk factors for coronary artery disease. Circ. Res. 89, E1–E7.

Yancopoulos, G.D., Davis, S., Gale, N.W., *et al*. (2000). Vascular-specific growth factors and blood vessel formation. Nature 407, 242–248.

Yao, Y.Y., Yin, H., Shen, B., *et al*. (2007). Tissue kallikrein and kinin infusion rescues failing myocardium after myocardial infarction. J. Card. Fail. 13, 588–596.

Yao, Y.Y., Yin, H., Shen, B., *et al*. (2008). Tissue kallikrein promotes neovascularization and improves cardiac function by the Akt-glycogen synthase kinase-3β pathway. Cardiovasc. Res. 80, 354–364.

Yao, Y.Y., Li, Y., Ma, G., *et al*. (2011). In vivo magnetic resonance imaging of injected endothelial progenitor cells after myocardial infarction in rats. Mol. Imaging Biol. 13, 303–313.

Yin, H., Chao, L., and Chao, J. (2005). Kallikrein/kinin protects against myocardial apoptosis after ischemia/reperfusion via Akt-glycogen synthase kinase-3 and Akt-Bad.14-3-3 signaling pathways. J. Biol. Chem. 280, 8022–8030.

Yoshida, H., Zhang, J.J., Chao, L., and Chao, J. (2000). Kallikrein gene delivery attenuates myocardial infarction and apoptosis after myocardial ischemia and reperfusion. Hypertension 35, 25–31.

Zhang, J.J., Chao, L., and Chao, J. (1999). Adenovirus-mediated kallikrein gene delivery reduces aortic thickening and stroke-induced death rate in Dahl salt-sensitive rats. Stroke 30, 1925–1931.

Address correspondence to:
Dr. Yu yu Yao
Department of Cardiology
Zhongda Hospital
Medical School of Southeast University
87 Dingjiaqiao
Nanjing, Jiangsu 210009
China

E-mail: yaoyuyunj@hotmail.com

Received for publication July 15, 2011;
accepted after revision March 6, 2012.

Published online: March 22, 2012.